



# A process-oriented scale-up/scale-down strategy for industrial blown film processes: Theory and experiments

Journal of Plastic Film &amp; Sheeting

2018, Vol. 34(3) 324–349

© The Author(s) 2017

Reprints and permissions:

[sagepub.co.uk/journalsPermissions.nav](http://sagepub.co.uk/journalsPermissions.nav)

DOI: 10.1177/8756087917741926

[journals.sagepub.com/home/jpf](http://journals.sagepub.com/home/jpf)

**Benedikt Neubert, Christoph Dohm,  
Johannes Wortberg and Marius Janßen**

## Abstract

To gain a competitive edge in developing innovative products, new multi-layer film manufacturers need to know whether laboratory-scale blown film line results reliably translate to large-scale production. This, however, is not always the case: Transferring process conditions and getting equal final film properties are not ensured. To address this problem, this paper presents a scale-independent scale-up/scale-down strategy to produce films with consistently similar properties regardless of a plant's size and design. A second aim is to prove this strategy is applicable by comparing the reference and experimental film mechanical properties. Here, experimental scale-down runs were carried out based on a process-oriented scale-up/scale-down strategy for the blown film process. An industrial production process (>800 kg/h), successfully transferred to a laboratory-scale blown film line, was used as the reference. The introduced process-oriented scale-up/scale-down is based on geometric and dynamic similarity. In this context, blow-up ratio, draw-down ratio and process time have been identified as major scale-up/scale-down variables. Unlike existing scale-up strategies, the process-oriented approach is more flexible in practice. Film mechanical properties taken from the experimental runs were determined by tensile and puncture resistance tests. The compared results confirmed that process-oriented scale-up/scale-down is feasible for the applied material and under the existing plant-

---

Faculty of Engineering, University of Duisburg-Essen, Duisburg, Germany

### Corresponding author:

Benedikt Neubert, Faculty of Engineering, University of Duisburg-Essen, Lotharstr. 1, Duisburg 47057, Germany.

Email: [Benedikt.Neubert@uni-due.de](mailto:Benedikt.Neubert@uni-due.de)

specific restrictions. The comparison indicated that most film properties produced on the laboratory-scale plant were comparable to those from the high-capacity blown film line.

### **Keywords**

Scale-up, scale-down, blown film process, film properties, process time, process oriented

## **Introduction**

The blown film process is a very important polymer-processing operation. Due to simultaneous machine direction (MD) and circumferential direction (CD) stretching, specific properties, such as directional strength or elasticity, can be altered. However, the final film properties are affected by different process variables. Furthermore, these variables strongly interact with each other, making the blown film process even more complex. Depending on the polymer material characteristics, the final film is a function of all prevailing influences. For the final solid film properties, it is essential to consider all these influences.

To stay competitive on international markets, it is crucial that manufacturers, especially those located in countries with high labor costs, continuously develop new and innovative products. New multi-layer structured film development is usually carried out on laboratory-scale blown film lines, primarily because less polymer is needed and the testing is faster. Meeting defined requirements regarding mechanical, optical or haptic properties represents the starting point for transferring to large-scale blown film lines. Scientifically, transferring operating conditions for manufacturing a film with defined and comparable properties between two differently scaled blown film lines is called scale-up or scale-down, respectively.<sup>1</sup> From the manufacturer's point of view, it would be helpful to accurately predict how a production line will perform in advance, thereby avoiding machine-downtime and minimizing waste.

Thus, beginning in the 1980s and during the ensuing 30 years, different strategies have been developed and examined to ensure that process conditions and final film properties transfer from a lab line to production. Based on the idea of obtaining equal film properties, various publications revealed the potentials of scale-up strategies. Nevertheless, in recent years, the scientific interest in this topic has waned. Furthermore, none of these strategies has yet been applied on high-capacity blown film lines, possibly because of their inflexibility and the fact that plant-specific constraints are not adequately considered. After all, it can be assumed that the practical application becomes even more challenging, the greater the plants differ in size. Consequently, the notion of a scale-independent transfer of process conditions and film properties is not ensured.

This paper aims to pick up the scientific discussion again. Therefore, a fully recorded industrial reference process, exceeding 800 kg/h, is the basis for this investigation. The goal is twofold: One is to provide a process-oriented and flexible scale-up/scale-down strategy which should ensure transferring process conditions and film properties among plants with significant differences in size and technical equipment. Plant-specific constraints such as mass flow rate limitations or the haul-off speed (laboratory-scale) need to be considered. A second goal is to prove the applicability of the presented strategy by extensively comparing the film mechanical properties, taken from the referenced industrial production process and from the experimental runs carried out on a laboratory-scale machine.

### Basic scale-up/scale-down strategies

Based on the bubble formation fundamentals described by Pearson and Petrie,<sup>2,3</sup> scale-up principles have been developed over the years. Initially, Pearson<sup>4</sup> stated some basic ideas in 1985. Upon testing new material compositions, the question arose about how the experimental findings on a laboratory-scale blown film line (subscript: lab) can be transferred to a larger production plant (subscript: pro). According to Pearson, a geometrical similarity between two differently scaled processes is necessary and achievable, meeting three requirements

$$BUR = \frac{d_{f,lab}}{d_{0,lab}} = \frac{d_{f,pro}}{d_{0,pro}} = \text{const.} \quad (1)$$

$$DDR = \frac{v_{f,lab}}{v_{0,lab}} = \frac{v_{f,pro}}{v_{0,pro}} = \text{const.} \quad (2)$$

$$x_{f,lab} = x_{f,pro} \quad (3)$$

where

$BUR$	=	blow-up ratio
$DDR$	=	draw-down ratio
$d_0$	=	die diameter (mm)
$d_f$	=	bubble diameter at the frost line (mm)
$v_0$	=	delivery rate of the melt (m/min)
$v_f$	=	film velocity at the frost line (m/min)
$x_f$	=	frost line height (m)

In addition, the height-dependent temperature profiles on the inner and outer bubble surfaces should be comparable. Nevertheless, besides the basic ideas, no further information is given about how to adjust individual parameters such as the mass flow rate or the haul-off speed for obtaining similar process states.

Subsequently, Kanai et al.<sup>5</sup> developed the first applicable scale-up strategy for the blown film process. Their primary strategy is to keep the bubble's maximum stresses in MD and CD identical. By achieving that, transferring the process states between two differently sized plants should be possible. A useful formal mathematical description of the scale-up strategy, derived by Kanai et al., is presented by Sukhadia.<sup>6</sup> The ratios between the die diameters and the die gap widths  $h_0$  represent the so-called scale-up ( $k > 1$ ) or scale-down ( $k < 1$ ) factors  $k$  and  $s$  which can be calculated as follows

$$k = \frac{d_{0,pro}}{d_{0,lab}} \quad (4)$$

$$s = \frac{h_{0,pro}}{h_{0,lab}} \quad (5)$$

Furthermore, the *BUR* (equation (1)), the *DDR* (equation (2)) and the frost line height ratio (equation (6)) have to be fulfilled

$$\frac{x_{f,lab}}{r_{0,lab}} = \frac{x_{f,pro}}{r_{0,pro}} = \text{const.} \quad (6)$$

where

$r_0$	=	die radius (mm)
-------	---	-----------------

Taking equations (1) and (2) and equations (4) to (6) into account and providing equal melt temperatures at the die gap for both plants, similar films can be produced by adapting relevant process parameters as follows<sup>1,6</sup>

$$\dot{m}_{pro} = k^2 \cdot s \cdot \dot{m}_{lab} \quad (7)$$

$$v_{f,pro} = k \cdot v_{f,lab} \quad (8)$$

$$h_{f,pro} = s \cdot h_{f,lab} \quad (9)$$

The bubble diameter at the frost line height, the melt delivery rate from the die gap and the frostline height for the production unit become

$$d_{f,pro} = k \cdot d_{f,lab} \quad (10)$$

$$v_{0,pro} = k \cdot v_{0,lab} \quad (11)$$

$$x_{f,pro} = k \cdot x_{f,lab} \quad (12)$$

where

$h_f$	=	film thickness at the frost line ( $\mu\text{m}$ )
$\dot{m}$	=	mass flow rate (kg/h)

Different papers<sup>5-7</sup> demonstrated that this scale-up/scale-down strategy is applicable for the many experimentally tested materials (e.g. different polyethylenes), extruder sizes, die diameters and further process variables. Table 1 summarizes the operating conditions investigated.

**Table 1.** Spectrum of experimentally tested process variables.<sup>5-7</sup>

Process variable	Value range
Die diameter (mm)	17–203
Dimensionless scale-up/scale-down factor $k$	1–7
Dimensionless scale-up/scale-down factor $s$	1–1.66
Mass flow rate (kg/h)	2–86.5
BUR	1.5–4.8
DDR	7–42

BUR: blow-up ratio; DDR: draw-down ratio.

Butler et al.<sup>8</sup> introduced an alternative scale-up strategy. These authors contend that the quadratic influence of the scale-up factor  $k$ , as shown in equation (7), leads to a disproportional change in the mass flow rate. Thus, they recommended considering the die geometry constraints by keeping the die-specific output rate (DSO) constant. It is defined as follows (European definition)

$$DSO = \frac{\dot{m}}{d_0} \quad (13)$$

(The American DSO definition multiplies the diameter  $d_0$  by  $\pi$ .)

As a result, the scale-up/scale-down factor  $k$  affects the mass flow rate linearly

$$\dot{m}_{pro} = k \cdot \dot{m}_{lab} \quad (14)$$

In addition, they introduced the dimensionless fabrication time ratio (FTR) as the polymer-specific relaxation time  $\lambda$  divided by the process time  $t_P$ , which allows characterizing the dynamic processes within the bubble formation zone. However, especially for multi-layer films, determining a proper  $\lambda$  is difficult. Once again, the BUR (equation (1)), the DDR (equation (2)) and also the FTR (equation (15)) need to be constant.

$$FTR = \frac{\lambda}{t_P} \quad (15)$$

The term ‘process time’ is the period for one small film element to move from the die gap to the frost line. Assuming a linear film velocity profile, the process time can be calculated as follows

$$t_P = \frac{x_f}{v_f - v_0} \cdot \ln\left(\frac{v_f}{v_0}\right) = \frac{x_f}{v_f - v_0} \cdot \ln(DDR) \quad (16)$$

Here, determining the melt delivery rate and the film velocity at the frost line height is based on the mass conservation principle (equation (17))

$$\dot{m} = 2\pi \cdot r \cdot h \cdot v \cdot \rho \quad (17)$$

where

$\rho$	=	density (kg/m <sup>3</sup> )
$r$	=	bubble radius (m)
$h$	=	film thickness ( $\mu\text{m}$ )
$v$	=	film velocity (m/min)

Additional requirements involve a consistent; relaxation time, melt temperature and die gap width for both scales ( $s=1$ ). Since the cooling conditions considerably affect how orientation and crystalline morphology develops in the tubular film process, Butler et al. also discussed making it quantifiable. Therefore, dimensionless figures, such as the Nusselt number (equation (18)) and the Graetz number (equation (19)), are used<sup>1,9</sup>

$$Nu = \frac{\alpha \cdot d}{\kappa} \quad (18)$$

$$Gr = \frac{\dot{m} \cdot c_p}{\kappa \cdot L} \quad (19)$$

where

$Nu$	=	Nusselt number
$Gr$	=	Graetz number
$\alpha$	=	heat transfer coefficient (W/m <sup>2</sup> K)
$d$	=	diameter (m)
$\kappa$	=	thermal conductivity (W/mK)
$L$	=	characteristic length (m)
$c_p$	=	specific heat capacity (J/kgK)

Experimental investigations also confirmed the possibility to use the presented dimensionless figures for describing process states and, thus, as a general basis for performing a scale-up.<sup>9</sup>

## Process-oriented scale-up/scale-down strategy

### Basic approach

All presented scale-up strategies for the blown film process are based on the desire to maintain final film properties versus the plant's scale. Therefore, influencing parameters need to be systematically adjusted so that the occurring effects during bubble formation remain constant. As macromolecular biaxial orientation, which is primarily induced by stretching the bubble in MD and CD, strongly correlates with the film mechanical properties, it is essential to keep the BUR and DDR constant during scale-up/scale-down. This necessary condition is named 'geometric similarity'. Moreover, partially crystalline polymers, such as PE, show time- and temperature-dependent material behavior that cannot be neglected when analyzing the blown film process. At this point, bubble cooling becomes important, because it determines heat removal and the process time. Keeping processing conditions similar versus process time is called 'dynamic similarity'.

As described in the previous section, the scale-up strategy presented by Kanai et al. focuses on global geometric similarity, according to equations (1), (2) and (6). Additionally, Butler et al. suggest considering time-dependent effects by means of dimensionless FTR (equation (15)), Nusselt number (equation (18)) and Graetz number (equation (19)). What both scale-up strategies share, however, is that they calculate just one single process state assumed to be similar or to lead to similar film properties. Another drawback is that the resulting process state is fully determined, which means that there

is no degree of freedom that would allow further manual adjustment regarding any technical restrictions that might occur. Consequently, depending on the scale difference between the blown film lines, the scale-up or scale-down may not be practically feasible.

Against this background, the process-oriented scale-up/scale-down strategy (POSS) aims to provide sufficient flexibility. Therefore, a degree of freedom is introduced by making the mass flow rate a variable process parameter. By considering the disagreement between Kanai et al. and Butler et al. about the mass flow rate adjustment, this approach is expected to be reasonable. Nevertheless, geometric similarity is still ensured by keeping BUR and DDR constant. As mentioned above, process time is believed to be a key scale-up/scale-down parameter, especially in terms of dynamic similarity.<sup>10</sup> Assuming a linear film velocity profile, process time depends on the melt delivery rate, the film velocity at the frost line and the frost line height itself (equation (16)). Following the principles of mass conservation (equation (17)), film velocity and melt delivery rate, in turn, directly result from the mass flow rate under geometrical scale-up/scale-down conditions. Demanding consistency of the linearly approximated process time, the POSS can be formulated as follows (presented for scale-up)

$$\dot{m}_{pro} = w \cdot \dot{m}_{lab} \quad (20)$$

$$x_{f,pro} = \frac{w}{k} \cdot t_{p,lab} \cdot C_{lab} \quad (21)$$

$$C_{lab} = \dot{m}_{lab} \cdot \left( \frac{1}{d_{f,lab} \cdot h_{f,lab} \cdot \rho_{f,lab}} - \frac{1}{d_{0,lab} \cdot h_{0,lab} \cdot \rho_{0,lab}} \right) \cdot \left[ \pi \cdot \ln \left( \frac{d_{0,lab} \cdot h_{0,lab} \cdot \rho_{0,lab}}{d_{f,lab} \cdot h_{f,lab} \cdot \rho_{f,lab}} \right) \right]^{-1} \quad (22)$$

where

$w$	=	process-oriented scale-up/scale-down variable
$k$	=	scale-up/scale-down factor (equation (4))
$C$	=	scale-up/scale-down constant (m/s)
$\rho_0$	=	density at the die exit (kg/m <sup>3</sup> )
$\rho_f$	=	density at the frost line (kg/m <sup>3</sup> )

Here, the scale-up/scale-down variable  $w$  allows flexible adjustment of the mass flow rate. Consequently, the frost line height for the large-scale process depends on the variable  $w$  and the given parameters  $k$ ,  $t_p$  and  $C$ . The constant factor  $C$  represents the referenced process state and has to be calculated during scale-up/scale-down (equation (22)). This process-oriented strategy



allows one to identify a suitable process state within a process window. The feasible process states are limited by processing- and plant-specific constraints, for example, the maximum mass flow rate or the cooling capacity, which, in turn, determines the frost line height. Furthermore, the process states calculated according to the strategies of Kanai et al. and Butler et al., respectively, are suggested as theoretical boundaries for the value range of  $w$  at a given value for  $k$ . Figure 1 illustrates this concept. The dotted lines indicate additional process states that although theoretically possible are probably not feasible, because they exceed the boundaries defined by Kanai et al. and Butler et al. (grey lines). The black lines represent the process states calculated with the POSS. If no scale-up is performed, the initial process state will obviously remain unchanged ( $k=1$ ,  $w=1$ ) and equals the intersection point of the lower and upper boundary lines.

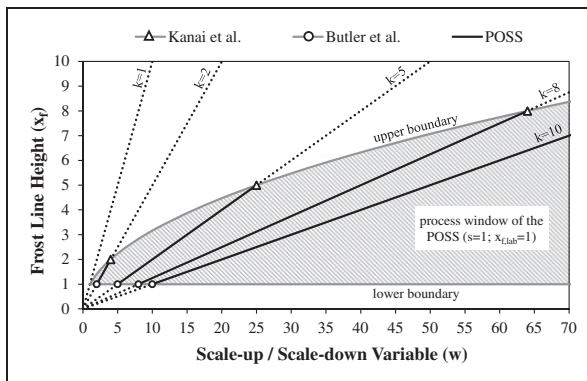


**Figure 1.** Exemplary comparison of scale-up strategies regarding calculated process states ( $x_f$  as function of  $w$ ) for different values of the scale-up factor  $k$  and  $x_f = 1$  as the initial state ( $w = 1$ ).

Finally, it should be mentioned that the POSS includes additional requirements in accordance with the approach presented by Butler et al., namely, the consistency of relaxation time, melt temperature, die gap width ( $s = 1$ ) and, thus, final film thickness.

As the process time is a key parameter, its determination should be as precise as possible. Therefore, the real bubble shape and the resulting velocity profile need to be considered. Both are influenced by material characteristics of the polymers used and the cooling conditions, such as the cooling air volumetric flow rate in combination with the installed cooling system (type of cooling ring, internal bubble cooling (IBC)). Consequently, a linear approximation is not necessarily appropriate, even though Butler et al. believe that the occurring error is less than 5%.<sup>8</sup> Provided that the real film

velocity profile and the bubble contour data are available in the form of  $v(x)$  and  $r(x)$ , respectively, the process time can be calculated approximately according to equation (23)

$$t_p = \sum_{i=1}^n \bar{v}_i^{-1} \cdot l_i \tag{23}$$

where

$\bar{v}$	=	average film velocity (m/s)
$l$	=	length of bubble segment (m)
$n$	=	number of segments
$i$	=	summation index for segments

Figure 2 illustrates the underlying approach, which follows Schmitz.<sup>11</sup> The bubble formation zone is divided into  $n$  small segments. For each segment, the residence time can be determined using a local average velocity  $\bar{v}_i$  and the bubble segment length  $l_i$ . The summation leads to the global process time. The finer the segmentation is, the more exact the calculation will be.

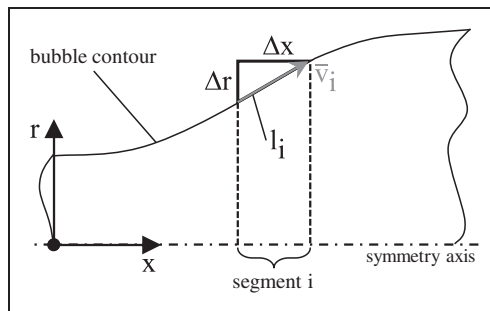


**Figure 2.** Bubble segmentation for calculating the process time.

The POSS accuracy increases, when real data for  $r(x)$  and  $v(x)$  are used. Instead of scaling the frost line height with a simplified linear process time (equation (16)), an approximation according to equation (23) should be taken into consideration. In general, analytically determining the frost line target position is thus no longer possible: it has to be done iteratively. Schmitz revealed that modifying certain process parameters, such as mass flow rate or frost line height, leads to a dilation or contraction of the bubble contour and the velocity profile, whereby their basic shape is not affected

significantly.<sup>11</sup> This means that both  $r(x)$  and  $v(x)$  can be adjusted to a certain extent by scaling a given master curve, which is useful for the aforementioned iterative determination of the target process state during scale-up or scale-down.<sup>12</sup>

All in all, the process-oriented strategy facilitates the practical scale-up/scale-down under given processing and plant-specific restrictions. The required flexibility is maintained by introducing a degree of freedom regarding the target process parameters. In accordance with other scale-up strategies, geometric similarity and dynamic similarity are still ensured. Since real bubble contour data and the film velocity profile are considered, the approach becomes more accurate.

### *Limitations of scale-up/scale-down strategies*

Basically, final film properties represent the overall outcome of the entire blown film process, which includes numerous steps such as melting the raw material in the extruder, forming the bubble at the extrusion die and within the bubble formation zone and post-treatment like additional stretching or surface treatment. Thus, films with equal properties produced at different plants imply a global similarity between the underlying processes. Accordingly, it is believed that the most promising strategy to perform a scale-up/scale-down is to provide similar processing conditions for each step, so that every conceived polymer element, hypothetically, experiences the same 'history' during its transformation from raw material to viscous melt and, finally, to solid film. At this point, the demand for a local similarity rises, meaning that the conceived element has a similar physical state at a defined position in the process independent of the plant. Clearly, completely realizing this ideal concept is impossible due to existing constraints in a production environment as well as in a laboratory.

In this context, the scale-up/scale-down question of the blown film process focuses on the bubble formation zone, starting at the die exit and ending at the frost line. Therefore, the fundamental assumption is that the polymer melt at the die exit is well defined according to the following conditions:

- the melt temperature is known and homogeneously distributed,
- the material is thermally and rheologically stable,
- the melt delivery rate is constant at any die gap position,
- extrudate-swelling phenomena are neglected,
- the macromolecules are oriented similarly, primarily in flow direction (MD),
- stresses due to shear flow in the spiral mandrel die are comparable,
- the melt is homogeneously mixed, and
- surface interactions between the melt and the die coating are neglected.

In the bubble formation zone, biaxial stretching and cooling take place simultaneously. Regarding local similarity, comparable MD and CD strain

rates as well as comparable heat transfer coefficients at the inner and outer bubble surface as functions of height above the die exit are desired. Here, the feasibility strongly depends on the plant-specific cooling system. In particular, using an IBC system has a significant impact, because the additional inside air stream causes a pressure profile along the bubble surface and thus affects local strain rates. What's more, the heat transfer is intensified and may vary locally.

## Experimental

Our non-disclosure agreement requires that no precise polymer information (e.g. MFI or solid-state density) be provided. Additionally, relevant process parameters are mostly stated in a dimensionless form.

### *Materials*

According to the stated goal of producing films with similar properties, the same composition was used for all experimental investigations. The extruded multilayer film has a symmetric three-layered structure. Each layer is a blend containing two different polyethylenes and a masterbatch. As will be shown, having precise information about the temperature-dependent material characteristics is very important. Therefore, the caloric data such as the thermal conductivity, the specific heat capacity and the specific volume (density) were measured.

### *Equipment*

As described earlier, for the scale-up/scale-down experiments, a high-capacity blown film line was used with maximum throughputs  $>800$  kg/h. The extrusion equipment included three 90 mm/32:1 L/D extruders and a three-layer spiral mandrel die with a diameter  $>600$  mm. For cooling the tubular film, a single-lip cooling ring and an IBC system were installed which, in turn, were fed by prechilled cooling air. The entire extrusion line was fully automated, using systems controlling the film thickness distribution, the blow-up ratio, the film width and the mass flow rate. Furthermore, devices for additional infrared heating and corona treatment were available.

The laboratory-scale blown film line was neither fully automated nor had prechilled cooling air. Therefore, the cooling air temperature was about equal to the ambient temperature. A single-lip cooling ring was used. In addition, no IBC was installed. For providing the requested mass flow rate, up to six extruders (25 mm/25:1 L/D and 30 mm/30:1 L/D) were used which, in turn, fed the spiral mandrel coextrusion die.

## Procedure

For this research, no classic scale-up was performed. Instead, a fully recorded process state on the high-capacity blown film line was selected as a starting point for a scale-down. Thus, high-resolution bubble images were taken and transformed into  $x$ - $r$  contour data according to a validated technique.<sup>13–15</sup> Measuring the material- and height-dependent film velocity profile is deemed to be important, too. By using a laser surface velocimeter (InteliSENS SL mini 3600, Co. Proton Products International Ltd), the local film velocities along the bubble were measured within  $\pm 0.05\%$  and a reproducible to  $0.02\%$ .<sup>16</sup> The film's temperature and pressure profiles were computed by integrating the contour data, the velocity profile and further process parameters into a numerical simulation. The numerical simulation includes a CFD analysis coupled with a contour calculation. For both laboratory-scale and industrial-scale blown film lines, the applicability of the procedure has been proven and, hence, will not be described here.<sup>11,13</sup>

As a next step, target process parameters for six different process states on the laboratory-scale blown film line were calculated, applying the introduced POSS. The scale-up factors  $k$  (equation (4)) and  $s$  (equation (5)) were 10 and 1, respectively. Since the scale-up/scale-down strategy predefines the frost line position, it is helpful to examine whether the demanded frost line height can be adjusted with the installed cooling configuration in advance. Therefore, different cooling parameters, including the volume flow rate and the cooling air temperature, were simulated by means of the aforementioned numerical procedure.

Apart from the systematically calculated processing conditions, an additional process state was considered, which was based on the machine operator's experience. Consequently, no explicit scale-down strategy, specifying neither the processing parameters nor the die gap size, was applied. All seven process states were experimentally carried out in the laboratory-scale plant. Finally, film samples were measured and their mechanical properties were compared among themselves and with the samples taken from the referenced production process according to DIN EN ISO 527–3 (tensile properties) and DIN EN 14477 (puncture resistance).

## Results and discussion

### Industrial process state

Figure 3 compares the experimentally recorded film contour to the simulated film contour (based on the mentioned numerical procedure). The figure includes an experimental contour approximation (Bézier Curve) starting at  $\sim 0.3$  dimensionless height. Below this height, the recording is impossible because the cooling ring covers the bubble. By contrast, the numerical

procedure can describe the complete bubble formation zone and beyond. Moreover, existing phenomena like the Venturi Effect can be simulated on a physically correct basis. The corresponding frost line heights are also indicated. The maximum deviation between the bubble radii is  $<2$  cm. Due to the measured caloric data, the observed and simulated frost line heights are very similar too.

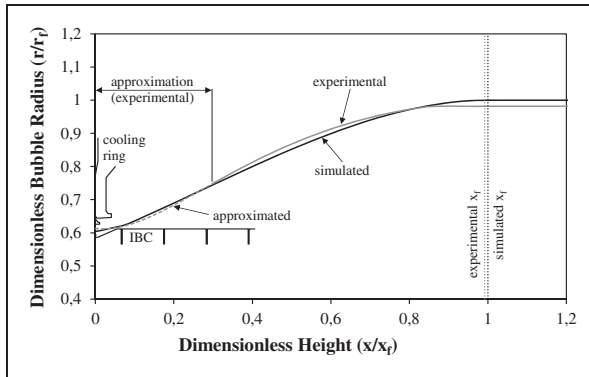


**Figure 3.** Dimensionless bubble radius vs. dimensionless height: Measured and simulated bubble radii and frost line heights for the reference process state.

Figure 4 presents the measured and calculated (polynomial function) local film velocities versus the dimensionless frost line height for the film produced under industrial processing conditions. The bars indicate the lowest and highest velocity measured for each point.

To ensure a good recording (quality value (QV)  $>60\%$ ), the measurement quality was continuously monitored. The cooling ring inhibited the measurement below  $\sim 0.4$  dimensionless frost line height. The melt ( $v_0$ ) delivery rate was calculated based on mass conservation (equation (17)). Nevertheless, it is noteworthy that the melt temperature could not be measured for the production plant. This would have required measuring the melt core temperature under production conditions (mass flow rate, switched-off cooling systems), which was not feasible. Hence, the melt temperature exiting the die was approximated using the prevailing backpressure inside the system. As a result, the melt temperature was set to  $195^\circ\text{C}$  which, in turn, is equal to the melt temperature exiting the laboratory-scale blown film line die. The laboratory-scale plant melt temperature was measured using a Type K thermocouple thermometer accurate to  $\pm(0.2^\circ\text{C} + 0.5\%)$ . For determining the process time, the simulated contour and the approximated film velocity profile were used. The presented calculation

method (equation (23)) leads to a 5.1-s process time. In contrast, equation (16) (linear approximation) leads to a 3.4-s process time, which equals a 33% deviation. Hence, equation (23) is assumed to be more precise for calculating the process time.

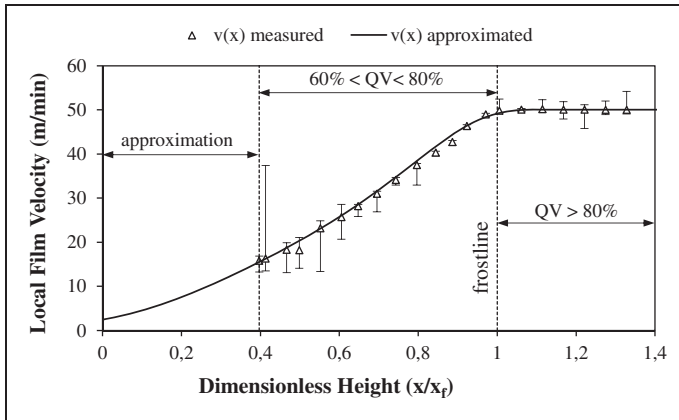


**Figure 4.** Local film velocity vs. dimensionless height: measured and approximated film velocity profiles for the industrial process state (run 0:  $\dot{m} > 800$  kg/h;  $d_0 > 600$  mm).

To demonstrate that POSS is better, it is necessary to take a closer look at the existing strategies. To that end, a theoretical scale-down from the industrial process state (run 0) was conducted with the scaling strategies proposed by Kanai et al. and Butler et al. Previously knowing the laboratory-scale blown film line constraints reveals their process-oriented limitations. A frost line height recording is limited to a minimum 0.105 m height; otherwise, the installed cooling ring would cover the frost line. Applying the scale-up strategy proposed by Kanai et al. would result in one single process state with a frost line height equal to 0.0937 m. However, this does not mean that applying this proven scaling strategy would not result in a film with desired film properties. If the scaling strategy published by Butler et al. were used, plant-specific constraints like the extruder capacities and the haul-off speed would become relevant. Referring to the industrial process state, the DSO would be 1.185 kg/hmm according to equation (13). This would be two times the maximal possible 0.544 kg/hmm DSO.

### *Applying the POSS strategy*

As stated above, six different process states with the target process parameters were calculated, based on the POSS. Table 2 summarizes the processing

conditions and the experimentally recorded data for both scales. This includes:

- DSO
- BUR
- DDR
- cooling conditions (cooling air temperature  $T_{air}$ , volume flow rate  $\dot{V}_{air}$ )
- melt temperature  $T_m$
- ratio  $i_h$  (target film thickness at the frost line height divided by the film thickness at the die gap)
- calculated frost line heights ( $x_{f,cal}$ ) for the lab-scale blown film line (runs 1–6)
- simulated frost line height for the production line ( $x_{f,cal}$ )
- experimentally recorded frost line heights ( $x_{f,exp}$ )

**Table 2.** Processing conditions for the reference process state (run 0), for the calculated process states (runs 1–6) and the experience-based process state (run 7).

	DSO (kg/hmm)	BUR –	DDR –	$T_{air}$ (°C)	$\dot{V}_{air}$ (m <sup>3</sup> /h)	$T_m$ (°C)	$x_{f,cal}$ (m)	$x_{f,exp}$ (m)	$i_h$ –	$t_p$ (s)
Run 0	1.1875		20.4	20 (22)	4,422 (1,263)		0.937	0.930		
Run 1	0.125 w=0.011		16.7		294.6		0.107	0.110		
Run 2	0.150 w=0.013	1.66	16.7		385.4		0.129	0.135		
Run 3	0.188 w=0.016		16.6	26.6	432.1	195	0.163	0.167	0.026	5.1
Run 4	0.225 w=0.019		17.3		456.7		0.196	0.186		
Run 5	0.263 w=0.022		17.5		459.6		0.230	0.238		
Run 6	0.313 w=0.026		16.9		433.2		0.275	0.276		
Run 7	0.1875		8.8	24.4	349.5	180	–	0.210	0.052	5.5

BUR: blow-up ratio; DDR: draw-down ratio; DSO: die-specific output rate.

As Table 2 shows, the DSO rates differ between 0.125 and 0.313 kg/hmm for runs 1–6. The DSO for the industrial process state is set to 1.1875 kg/hmm. The BURs are nearly constant for both scales, and the layflat width is well controlled. Compared to the reference process state (run 0), the DDRs for the experimental investigations (runs 1–6) are lower, which seems to be a



systematic deviation. Since the DDRs should have been the same, this fact cannot be neglected. Nevertheless, in order to compare the final film properties, approaching the target film thickness was more important. Taking a closer look at both scales reveals the differences in the cooling conditions. According to industrial standards, both an external and internal cooling system were used for the reference process, thereby providing 4422 m<sup>3</sup>/h (cooling ring) and 1263 m<sup>3</sup>/h (IBC) mean volume flow rates. The internal volume flow was portioned in a single tangential and four radial flows. Additionally, the cooling air was precooled to 20°C (cooling ring) and 22°C (IBC). As usual for a laboratory-scale blown film line, no IBC was available. Thus, the external cooling air correlated to the ambient temperature. As a further requirement for the scale-down, the melt temperature exiting the die was set to 195°C for both processes. Furthermore, Table 2 clearly reveals that the difference between the calculated and experimentally recorded frost line heights are minor (runs 1–6). By applying the POSS, the process time  $t_p$ , as an indicator for dynamic similarity, was expected to be 5.1 s for all experiments. To prove this, the process time was recorded for one process state (run 2), using a known technique.<sup>7,17</sup> First, the bubble was marked with a viscous paint close to the die gap. Passing the bubble formation zone, the paint progress was recorded with a video camera. Knowing the shutter speed and playing back the recording frame-by-frame resulted in a measured 5.4 s process time, which is in very good agreement with the calculation. Table 2 also reports the settings for the experienced-based process state (run 7). One sees that the DDR is almost half the target DDR, and the melt temperature is 15°C lower. Another difference is that the applied die gap was half the production process and the final film thickness was kept constant.

### *Mechanical properties*

When comparing mechanical properties in general, one must consider the measured film thickness instead of the target film thickness. To improve the statistical comparison, 10 samples in MD and CD were measured for each run. The following figures contain the value  $\tilde{h}$ , which is the averaged measured sample thickness divided by the target thickness. The vertical error bars correspond to a 95% confidence limit with respect to the testing error. For the measurements, the maximum measuring error is  $\pm 0.3\%$  for the force transducer and  $\pm 0.15\%$  for the extensometer, respectively.

Figures 5 and 6 show the MD and CD modulus of elasticity for all conducted runs. Based on the measuring procedure and because the film thicknesses varied, the samples in machine and CD cannot be correlated. The modulus of elasticity was measured as the secant modulus between 0.75% and 1.25% of elongation. The data show that the modulus for runs 1–6 in MD is always higher than the modulus for the reference process state; the same is true for the experienced-based run. Statistically, the average modulus

of all films produced under scale-up/scale-down conditions is almost 20% higher. However, one sees that a considerable reproducibility could be achieved. In comparison, the modulus for run 7 deviates by nearly 32% from the reference process.

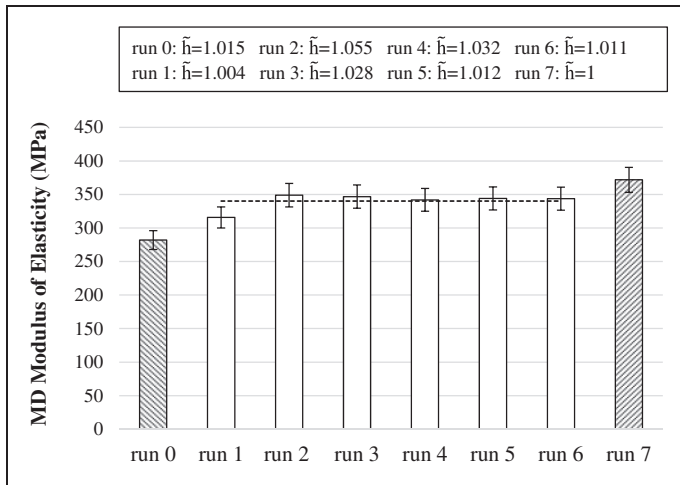


**Figure 5.** MD modulus of elasticity for the reference process state (run 0), for the calculated process states (runs 1–6) and the experience-based process state (run 7). The dotted line is the average value for runs 1–6.

For both the production and the laboratory process, the CD modulus is higher than the MD modulus, which corresponds to the typical findings in literature.<sup>18–20</sup> However, a closer look at the required mechanical product specifications confirms a higher CD modulus and similarly for the tensile stress at yield in axial and CD. Hence, the typical anisotropic properties for blown films not only depend on the processing conditions but are also defined by the product requirements, requested by the client. The difference between the averaged value (runs 1–6) and the reference process state is just 5%, which is similar to the results from the experience-based process state. Moreover, variations among runs 1–6 are observed. Possible reasons for this are many. Deviations may be attributed to a non-existent thickness control system and die centering or film cooling asymmetries. The average standard deviation for all film sample thicknesses (runs 1–6) is 4.5  $\mu\text{m}$ , compared to a standard deviation of 1.1  $\mu\text{m}$  for the reference process. Possible thickness variations, in turn, can result in an inhomogeneous film stretching, which may cause the larger deviations in run 1 and run 3.

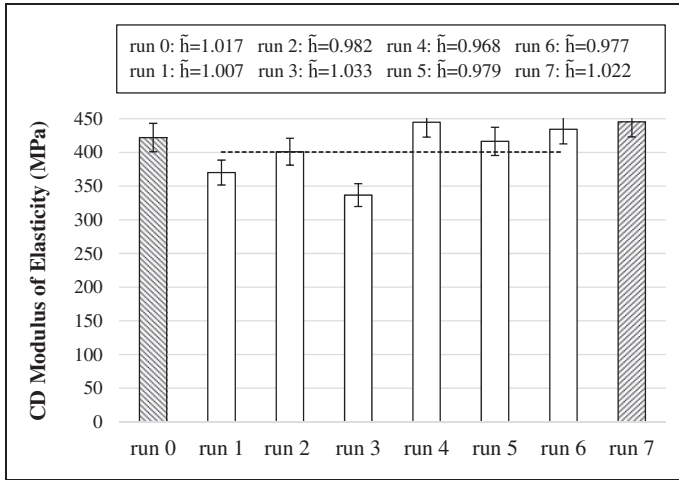


**Figure 6.** CD modulus of elasticity for the reference process state (run 0), for the calculated process states (runs 1–6) and the experience-based process state (run 7). The dotted line is the average value for runs 1–6.

As a further customer requirement, the MD and CD tensile stresses at yield have to be in a specified tolerance. Figures 7 and 8 show the tensile stresses at yield for runs 0–7. For both processes, the average CD stresses are somewhat higher than in MD or nearly comparable. A possible explanation may be that the BUR is high enough to compensate for the differences in the molecular orientation (longitudinal to transverse orientation ratio), which again depends upon the polymer and process. In addition, the specific polymer properties may have a larger impact and, thus, compensate the processing influences.

According to the designated goal of the POSS, still a very good reproducibility for all calculated process states has been achieved in MD (Figure 7). Furthermore, runs 1–6 tend to confirm the run 0 values better than run 7. For both directions, however, the reference sample mean exceeds runs 1–6 and 7. Table 2 shows that the DDR for run 0 is higher than the DDR for runs 1–6. Thus, the higher MD stresses might indicate a higher longitudinal orientation due to more stretching and, hence, a change in morphology. This has been observed in numerous publications.<sup>21,22</sup> Despite clear differences in the induced material stresses (shear stresses in the extruders/spiral mandrel coextrusion die) and in the cooling conditions, the degree of crystallinity did not change significantly for both process scales, which was measured by differential scanning calorimetry. Especially for partially crystalline polymer films, it is known that the mechanical properties are more affected by the induced orientations than by the degree of crystallinity.<sup>23,24</sup> Nevertheless, this does

not mean that crystalline characteristics such as the crystal sizes are similar, because the crystallizing conditions are different.

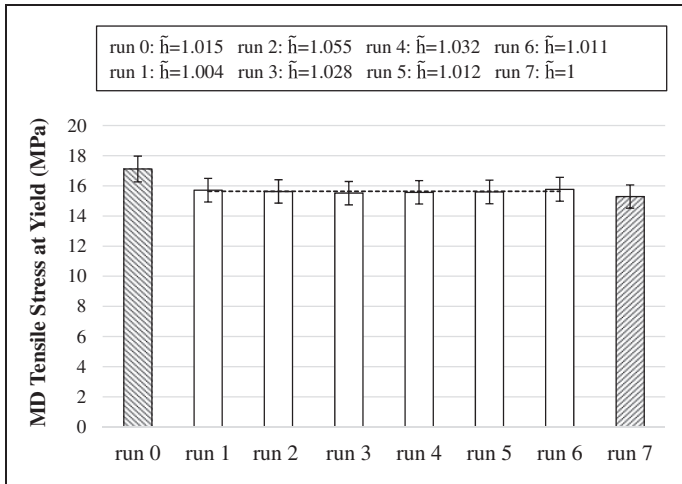


**Figure 7.** MD tensile stress at yield for the reference process state (run 0), for the calculated process states (runs 1–6) and the experience-based process state (run 7). The dotted line is the average value for runs 1–6.

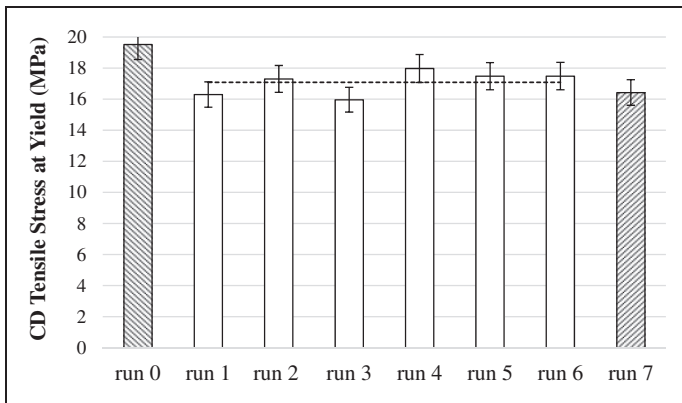


**Figure 8.** CD tensile stress at yield for the reference process state (run 0), for the calculated process states (runs 1–6) and the experience-based process state (run 7). The dotted line is the average value for runs 1–6.

Comparing the average MD stress for runs 1–6 to run 7 shows that the difference is within the statistical uncertainty, despite a much lower DDR. A possible explanation may be how melt orientation in the narrower die gap (run 7) influences the mechanical properties.

Higher observed CD tensile stresses for run 0 (Figure 8) may be attributed to the installed IBC device. The effect of the resulting pressure load on the inner film surface is twofold: One concerns the impinging first volume flow (cooling air) which causes a higher pressure load than the inner static pressure for the laboratory-scale blown film line. In turn, this may result in early film stretching (close to the die gap) and higher transverse orientation, respectively. On the other hand, due to the active film cooling, these orientations or even different layers may become solidified in an earlier state. To clarify these phenomena, further morphological investigations would be necessary; yet, these are not a part of the presented work.

Figures 9 and 10 present the average elongation at break for all runs. One sees that the MD elongation is consistently higher than the CD elongation. Furthermore, the average for all samples (runs 1–6) in CD exceeds the elongation for run 0, which is the opposite for MD. Higher MD longitudinal orientations correlate with the DDR. As stated above, the applied process technologies affect the melt quality. For example, the machine component surface coatings in contact with the melt might cause structural defects which, in turn, would influence the elongation at break. Nevertheless, these findings correlate well with the reference state.

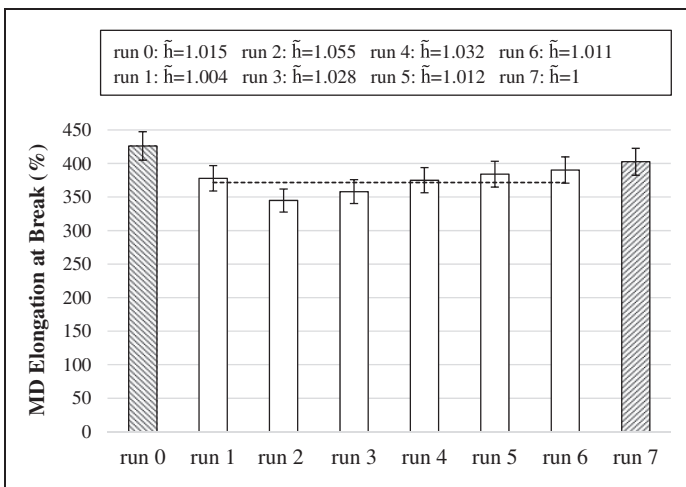


**Figure 9.** MD elongation at break for the reference process state (run 0), for the calculated process states (runs 1–6) and the experience-based process state (run 7). The dotted line is the average value for runs 1–6.

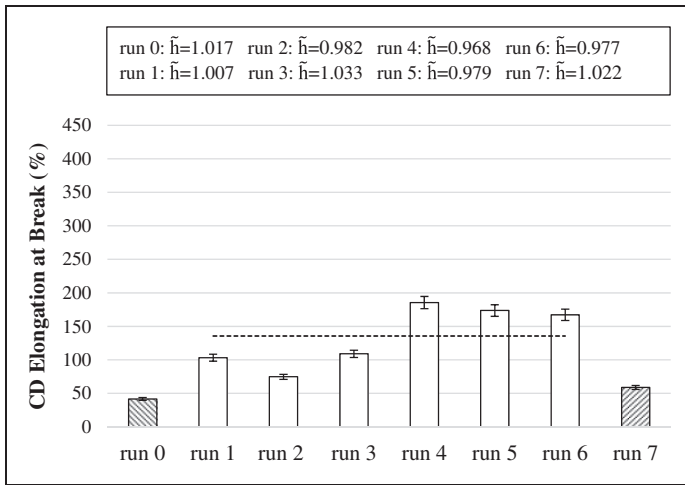


**Figure 10.** CD elongation at break for the reference process state (run 0), for the calculated process states (runs 1–6) and the experience-based process state (run 7). The dotted line is the average value for runs 1–6.

In addition, the puncture resistance, elongation and penetration energy were measured according to DIN EN 14477. The puncture resistance measures the prevailing anisotropy ratio. It is expected that a higher anisotropy ratio leads to a lower puncture resistance. Figure 11 shows the results.

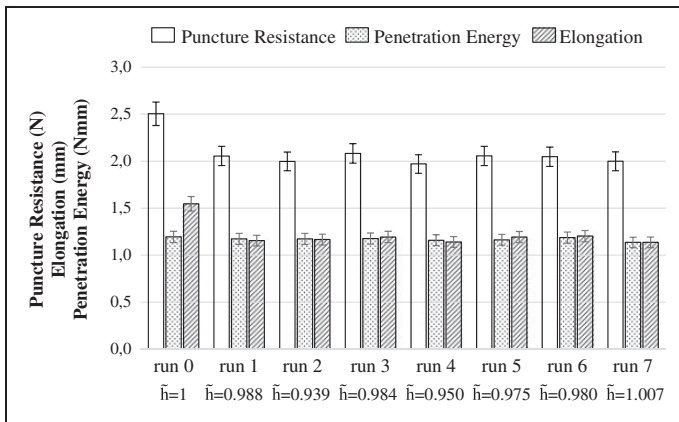


**Figure 11.** Puncture resistance, elongation and penetration energy for the reference process state (run 0), for the calculated process states (runs 1–6) and the experience-based process state (run 7).

Besides the average puncture resistance, the elongation and the penetration energy are stated with corresponding average film sample thicknesses. Regardless of the processing conditions for all calculated runs (runs 1–6), the results show a very good comparability. The processing conditions reported in Table 2 (BUR, DDR) indicate a higher anisotropy for run 0 compared to runs 1–7. The results in Figure 11 do not correspond to the expectations, as the puncture resistance should be lower. This might be attributed to the higher film thickness for run 0 than for runs 1–6, which might increase the puncture resistance.

## **Summary and conclusion**

In this work, a POSS strategy was introduced, providing higher flexibility in practical use. Applying this strategy, six different process states were calculated based on an industrial process state ( $>800$  kg/h), thus performing a scale-down. Subsequently, for all calculated process states, film samples were taken. The effect of processing conditions on the mechanical properties among the produced multi-layered film samples was studied and compared to the reference process and an experience-based process state. Then, characteristic values derived from tensile tests and puncture resistance tests were analyzed.

We demonstrated that the industrial process state was successfully scaled down using the process-oriented and flexible strategy. We further established that the scale-up/scale-down procedure is independent of the prevailing plant-specific constraints, ensuring more flexibility. Furthermore, results confirm that, for all calculated process states, a high reproducibility of the mechanical properties was achieved. Geometrical and dynamic similarity (local and global) within the bubble formation zone was mainly provided, thereby ensuring a transferability of process states and final film properties, independent of the plant scale. Furthermore, the film mechanical characteristics from the calculated process states appear to be more similar to the ones for the reference state, than the experience-based state. Based on the presented results, the feasibility of the process-oriented approach under the given processing conditions has been shown. It should be noted that the investigations were conducted for a relatively robust material composition.

Hence, further investigations should deal with a more sensitive product like a barrier film. Regarding the basic POSS principles, no changes are assumed to be required because the stated scale-up/scale-down conditions do not depend on the considered product. Nevertheless, this does not exclude measuring and using the caloric data and the film velocity profile, which ensures a correct material behavior representation. Moreover, additional product-dependent specifications like optical or haptic properties should be investigated. Beyond that, the cooling configuration for the laboratory-scale blown film line could be adapted. On the one hand, integrating an IBC has to

be considered. On the other hand, the cooling ring geometry (production plant) should be downscaled. With the described numerical procedure, possible potentials of these changes could be analyzed in advance. In particular, the interactions between the flow phenomena and the bubble can be simulated and evaluated regarding the geometrical and dynamic similarity.

### Declaration of Conflicting Interests

The author(s) declared no potential conflicts of interest with respect to the research, authorship, and/or publication of this article.

### Funding

The author(s) disclosed receipt of the following financial support for the research, authorship, and/or publication of this article: We would like to thank the German National Science Foundation (DFG) for funding our research.

### References

1. Michaeli W and Hauck J. Up-Scaling experimenteller Untersuchungsergebnisse von Labor- auf Produktionsanlagen. In: VDI-Gesellschaft Kunststofftechnik (eds) *Wertschöpfung bei der Folienextrusion*. Düsseldorf: VDI-Verlag, 1999, pp.165–199.
2. Pearson JRA and Petrie CJS. The flow of a tubular film. Part I: formal mathematical representation. *J Fluid Mech* 1970; 40: 1–19.
3. Pearson JRA and Petrie CJS. The flow of a tubular film. Part I: formal mathematical representation. *J Fluid Mech*. 1970; 42: 609–625.
4. Pearson JRA. *Mechanics of polymer processing*. London: Elsevier Applied Science Publishers, 1985, pp.508–510.
5. Kanai T, Kimura M and Asano Y. Studies on scale-up of tubular film extrusion. *J Plast Film Sheet* 1986; 2: 224–241.
6. Sukhadia AM. Scale-up and processing-structure-property analysis of the blown film process. *J Plast Film Sheet* 1994; 10: 213–234.
7. Simpson DM and Harrison IR. The use of deformation rates in the scale-up of polyethylene blown film extrusion. *J Plast Film Sheet* 1992; 8: 192–206.
8. Butler TI, Lai SY and Patel R. Scale-up factors effecting crystallization in polyolefin blown film. In: *TAPPI PL&C Conference*, Nashville, TN, USA, 1994, Atlanta, GA, USA: TAPPI Press, pp.289–305.
9. Butler TI. Using dimensionless scale-up variables to predict LLDPE blown film properties. In: *TAPPI PL&C Conference*, Chicago, IL, USA, 1995, Atlanta GA: TAPPI Press, pp.581–601
10. Shirodkar PP, Firdaus V and Fruitwala H. Scale-up of LLDPE blown film extrusion. In: *TAPPI PL&C Conference*, Nashville, TN, USA, 1994, Atlanta, GA: TAPPI Press, pp.405–413
11. Schmitz GJ. *Experimentelle Analyse und numerische Modellierung der Deformationsvorgänge bei der Schlauchfolienextrusion*. PhD Thesis, RWTH Aachen University, Germany, 1996.



12. Janas ML. *Eine neuartige numerische Methode zur Optimierung und Intensivierung der Blasfolienkühlung*. PhD Thesis, University of Duisburg-Essen, Germany, 2015.
13. Spigatis J. *Untersuchung des Einflusses des instationären konvektiven Wärmeübergangs bei der Folienherstellung auf die Produktqualität*. PhD Thesis, University of Duisburg-Essen, Germany, 2004.
14. Bussmann M. *Ein kalibrierbares integratives Modell zur Beschreibung des Schlauchbildungsprozesses in der Blasfolienextrusion*. PhD Thesis, University of Duisburg-Essen, Germany, 2010.
15. Hauck J. *Entwicklung eines Simulationsprogrammes für den Schlauchfolienextrusionsprozess*. PhD Thesis, RWTH Aachen University, Germany, 1999.
16. Proton Products. Series Brochure, IntelliSENS SL mini Series, 2017.
17. Huang TA and Campbell GA. Deformational history of LLDPE/LDPE blends on blown film equipment. *Adv Polym Technol* 1985; 5: 181–192.
18. Ohlendorf F. *Vorhersage der mechanischen Folieneigenschaften bei der Schlauchfolienextrusion*. PhD Thesis, RWTH Aachen University, Germany, 2004.
19. Tas PP. *Film blowing: from polymer to product*. PhD Thesis, Eindhoven University of Technology, Eindhoven, Netherlands, 1994.
20. Patel RM, Butler TI, Walton KL, et al. Investigation of processing-structure-properties relationships in polyethylene blown films. *Polym Eng Sci* 1994; 34: 1505–1514.
21. Han CD and Kwack TH. Rheology-processing-property relationships in tubular blown film extrusion. II. Low-pressure low-density polyethylene. *J Appl Polym Sci* 1983; 28: 3419–3433.
22. Kanai T. Theoretical analysis of tubular film extrusion and its applications for HMW-HDPE. *IPP* 1987; 1: 137–143.
23. De Vries AJ. Structure-properties relationships in biaxially oriented polypropylene films. *Polym Eng Sci* 1983; 23: 241–246.
24. Yamada K, Kamezawa M and Takayanagi M. Relationship between orientation of amorphous chains and modulus in highly oriented polypropylene. *J Appl Polym Sci* 1981; 26: 49–64.

## Biographies

**Benedikt Neubert** studied mechanical engineering at the University of Duisburg-Essen, Germany, with a specialization in thermal process engineering, earning a Master of Science degree in 2013. Since June 2013, he has been working as a research assistant at the Institute of Product Engineering (IPE) at the chair of Engineering Design and Plastics Machinery (KKM), University of Duisburg-Essen. Currently, he heads the Extrusion work group.

**Christoph Dohm** studied industrial engineering at the University of Duisburg Essen, Germany, with mechanical engineering and management as his field of study. Conferred the Master of Science degree in March 2017, he is now a research assistant at the Institute of Product Engineering (IPE) at the chair of

Engineering Design and Plastics Machinery (KKM), University of Duisburg-Essen.

**Johannes Wortberg** studied mechanical engineering at RWTH Aachen University, Germany, with a specialization in plastic technology, receiving his doctoral degree in December 1978. Since then until 1983, he worked as a research fellow and was head of the Extrusion and Injection Molding division at the Institute of Plastics Processing (IKV) at RWTH Aachen University. From April 1983 to December 1986, he worked at Battenfeld Extrusionstechnik GmbH, Bochum, Germany (today: BC Extrusion Holding GmbH) where he headed the Research and Development department and later became the plant manager. From January 1987 to December 1992, he was a university professor at the University Paderborn, Germany. Subsequently, from January 1993 to March 2000, he was a professor at the University Essen, Germany. Since January 2001, he has held the chair of Engineering Design and Plastics Machinery (KKM) at the Institute of Product Engineering (IPE) at the University of Duisburg-Essen. Since February 2017, he is a senior professor at the University of Duisburg-Essen.

**Marius Janßen** is doing graduate studies in mechanical engineering with a specialization in product engineering at the University of Duisburg-Essen, Germany, where he received his Bachelor of Science in 2016.

# DuEPublico

Duisburg-Essen Publications online

UNIVERSITÄT  
DUISBURG  
ESSEN

*Offen im Denken*

ub | universitäts  
bibliothek

This text is made available via DuEPublico, the institutional repository of the University of Duisburg-Essen. This version may eventually differ from another version distributed by a commercial publisher.

**DOI:** 10.1177/8756087917741926

**URN:** urn:nbn:de:hbz:465-20220921-153545-3

This publication is with permission of the rights owner freely accessible due to an Alliance licence and a national licence (funded by the DFG, German Research Foundation) respectively.

All rights reserved.